Hindawi
Wireless Communications and Mobile Computing
Volume 2022, Article ID 4139345, 13 pages
https://doi.org/10.1155/2022/4139345

Research Article

Cognitive-Based High Robustness Frequency Hopping Strategy for UAV Swarms in Complex Electromagnetic Environment

Rui Xue and Mingfei Zhao

Harbin Engineering University, Harbin 150001, China

Correspondence should be addressed to Mingfei Zhao; zhaomingfei0825@hotmail.com

Received 17 May 2022; Revised 19 June 2022; Accepted 7 July 2022; Published 31 July 2022

Academic Editor: Mingqian Liu

Unmanned aerial vehicles (UAVs) confront various interference in the process of missions, and frequency hopping (FH) technology is one of the effective means of anti-interference for UAV. The FH system can avoid interference frequency points and possess certain anti-interference ability by making the carrier frequency continuously popping. However, the increasingly complex electromagnetic environment of UAV swarms requires more efficient anti-interference measure. To further improve the anti-interference ability of UAVs, this paper proposes a cognitive-based high robustness FH strategy. By adding a cognitive module to FH system, UAVs can avoid the interference frequency points adaptively and sensitively. The proposed system can identify typical suppressed interference and filter the interference frequency points. Cognitive FH system can avoid interference points completely with accurate detections and enhance the robustness for UAV swarms in complex electromagnetic environment compared to conventional FH system. Simulation results have shown that BER performance of proposed cognitive FH strategy is better than conventional FH strategy for typical suppressed interference.

1. Introduction

The applications of unmanned aerial vehicles (UAVs) become more and more extensive in both civil and military fields due to advantages such as low cost, light weight and ease of deployment [1–5]. As the missions become more intricate, multiple UAVs as a swarm instead of one single UAV obtain wider applications [6–8]. However, as information technology and communication network are developing rapidly [9], the electromagnetic environment confronted by UAV swarms for wireless communication is more complex [10]. Multiple drones will face different geographical environment, weather environment, and electromagnetic environment when performing tasks [11]. Therefore, a high robustness system is the key of information transmission for UAV swarms. To guarantee the reliability and security of data transmission, the anti-interference ability of UAV swarm is increasingly required [12].

The data link of UAV swarms can be divided into uplink, downlink, and relay link due to the direction of information transmission, as shown in Figure 1. Uplink is mainly used to send control and command information. The amount of uplink information is small, and the time of transmission is short, which makes uplink data difficult to interfere [13]. Different from the uplink, the transmission of downlink data is easily interfered because downlink is primarily used to transmit multimedia information from UAVs such as high-definition images and videos, which occupy more transmission time. Specially, remote UAVs employ satellite relays to transmit data, which increases the risk of interference. For example, RQ-170 Sentinel UAV was captured by Iranian forces due to the interference signal on December 4, 2011 [14]. The external interference faced by UAVs can be divided into suppressed interference and deceptive interference [15]. Suppressed interference suppresses the source information by sending high-power

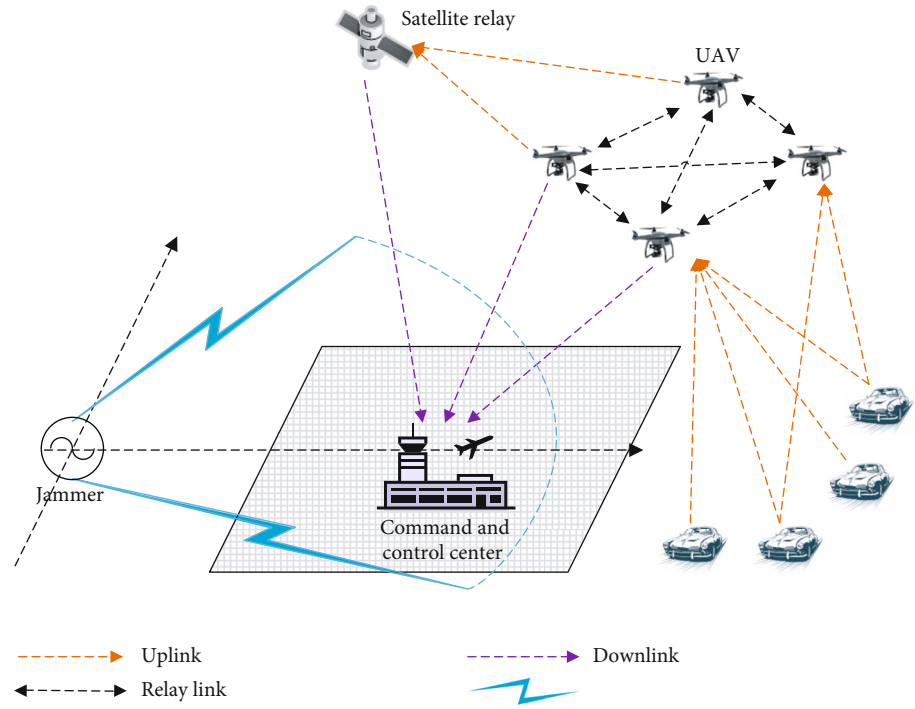

Figure 1: Types of UAV communication links.

interference, which is simple in implementation and has become a widely applied interference method recently. Therefore, the interference faced by downlink data of UAVs is mostly suppressed interference, including broadband noise (BN) interference [16], single-tone (ST) interference, multitone (MT) interference [17], narrowband noise (NN) interference [18], and linear frequency modulation (LFM) interference [19].

The anti-interference of UAVs is to taking certain measures to eliminate the influence of interference sources on UAV communications, so that UAV can complete data transmission [20]. Each anti-interference technology is effective to one or several certain interferences, and no existing anti-interference technology can resist all types of interference [21]. The anti-interference methods of UAVs mainly include direct sequence spread spectrum technology, frequency hopping (FH) technology, time hopping technology, hybrid spread spectrum technology, and adaptive antenna nulling technology [22]. Among them, FH technology is generally applied due to its excellent anti-interference performance and covert communication capability by continually changing the frequency point to avoid interference. Identification and detection of interference signals is the foundation of FH system. Improving the performance of detection and identification can enhance the anti-interference ability of the system [23, 24]. The authors in [25] employ a differential FH communication system for UAVs to confront interference and verify the performance of the system in Rician channels. However, the Rician channel model is not universal in UAV systems. The authors in [26] propose a reinforcement learning approach for antijamming communications in UAV swarms. This method has improved the communication quality, but the application of the scheme is limited due to its high complexity. The authors in [27] present a local reaction antijamming scheme based on adaptive frequency hopping. The FH strategy of the scheme is selected based on the node type without considering the type of interference.

We can observe that FH technology is an effective method for the anti-interference ability of one single drone. However, the advantages of FH diminish as the increasing number of UAVs due to the more complex electromagnetic environment. Conventional FH system simply carries out according to established rules without the ability of interference detecting. To further promote the robustness of UAV swarms, we propose a cognitive-based FH strategy for anti-interference in complex electromagnetic environment. The proposed strategy adds cognitive decision module compared to the conventional FH system and avoid the interference point in advance by interference detection algorithms. Cognitive FH strategy conforms to the development trend of UAV and provides crucial guarantee for the robustness of information transmission, which can meet communication requirements in complex electromagnetic environments.

The rest of the paper is organized as follows. Section 2 describes the interference detection algorithm, which is the basis of cognitive FH strategy. Section 3 expresses the cognitive FH strategy for UAV swarms, including the system model and functional module. Section 4 introduces the numerical results and analysis. Section 5 is the conclusions.

2. Interference Detection Algorithm

The interference of UAVs mainly comprises suppressed interference and deceptive interference. Suppressed interference is simpler to implement and becomes a common means

of interference, including BN interference, ST interference, MT interference, NN interference, and LF interference. For the five kinds of interference above, the interference signal model and interference recognition algorithm are introduced in this section.

2.1. Interference Signal Model. BN interference generates interference signals by employing random noise and applies them to all hopping subchannels. Therefore, additive white Gaussian noise (AWGN) is required to generate BN interference, which is shown as follows:

$$x_{\mathrm{BN}}(t) \sim N\left(0, \frac{P_J}{2W_s}\right), \tag{1}$$

where W_s and P_J present the bandwidth of the system and interference power. BN interference can be obtained by filtering Gaussian white noise as follows:

$$J_{\mathrm{BN}}(t) = \int_{-\infty}^{\infty} x(\tau)h(t-\tau)d\tau, \tag{2}$$

where the filter function is $h(t)$ and the Fourier transform of $h(t)$ is $H_{\mathrm{BN}}(j2\pi f)$, which can be expressed as follows:

$$H_{\mathrm{BN}}(j2\pi f) = \begin{cases} 1, & |f| \le W_s, \\ 0, & \text{else.} \end{cases} \tag{3}$$

Then, an amplifier is employed to generate BN interference, which is used to suppress the entire frequency band of the target system. The time domain diagram and frequency domain diagram of BN interference is shown in Figure 2 when the interference power is 8 dBW. BN interference is applied to the entire frequency band. Therefore, it is necessary to expand the bandwidth to improve the anti-interference performance.

NN interference uses narrowband filters to process Gaussian white noise, which is the difference between NN interference and BN interference. Gaussian white noise of NN interference can be expressed as follows:

$$x_{\mathrm{NN}}(t) \sim N\left(0, \frac{P_J}{2W_J}\right), \tag{4}$$

where W_J is the interfered bandwidth of the system. After the filter, NN interference is depicted as follows:

$$J_{\mathrm{NN}}(t) = \int_{-\infty}^{\infty} x(\tau)h(t-\tau)d\tau. \tag{5}$$

$H_{\mathrm{NN}}(j2\pi f)$ is the Fourier transform of $h(t)$, and $H_{\mathrm{BN}}(j2\pi f)$ is related to the bandwidth of the interference signal. $H_{\mathrm{BN}}(j2\pi f)$ can be expressed as follows:

$$H(j2\pi f) = \begin{cases} 1, & \left|f \pm f_J\right| \le \dfrac{W_J}{2}, \\ 0, & \text{else,} \end{cases} \tag{6}$$

where f_J and W_J denote the centre frequency and the bandwidth of the interference, respectively. The time domain diagram and frequency domain diagram of NN interference are depicted in Figure 2 when interference power is 8 dBW and the value of interference factor $k = 1$. Inaccuracy of threshold setting for forward consecutive mean excision (FCME) with single thresholds will affect the detection performance and FCME with double thresholds can avoid high probability of false alarm. Therefore, FCME with double thresholds is selected for NN interference.

ST interference and MT interference are both tone interference. The domain expression of the ST interference is as follows:

$$J_{\mathrm{ST}}(t) = \sqrt{2P_J}\cos\left(2\pi f_J t + \varphi\right), \tag{7}$$

where f_J and φ denote interference frequency and initial phase. ST interference imposes all power on the frequency point f_J with energy concentration but limited interference range. The time domain diagram and frequency domain diagram of ST interference when the interference power is 1 dBW are shown in Figure 2.

MT interference is the application of interference signal to some specific frequency points in the frequency hopping band. The domain expression of the MT interference is as follows:

$$J_{\mathrm{MT}}(t) = \sum_{i=1}^{N_J} \sqrt{2P_i}\cos\left(2\pi f_i t + \varphi_i\right), \tag{8}$$

where N_J is the number of interference points. The range of MT interference is larger than ST interference, and its interference frequency is more concentrated than NN interference. The time domain diagram and frequency domain diagram when interference is 1 dBW are shown in Figure 2.

In addition, the domain expression of LFM interference is shown as follows:

$$J_{\mathrm{LFM}}(t) = A\exp\left[j\left(2\pi f_j t + \pi K t^2 + \varphi\right)\right], \quad 0 \le t \le T, \tag{9}$$

where A is the signal amplitude, f_j is the centre frequency, φ is the initial phase, T is the signal duration, B_{LFM} is the frequency modulation interference bandwidth, and $K = B_{\mathrm{LFM}}/T$. The time domain diagram and frequency domain diagram are shown in Figure 2. The sampling frequency f_s = 1000Hz, the interference power is 1 dBW, and the sweep bandwidth is frequency domain diagram of LFM interference with 100M. For ST, MT, and LFM interference, to reduce the detection delay and improve the real-time performance of the detection algorithm, the single-threshold FCME algorithm is selected.

2.2. Interference Detection Algorithm. The interference detection algorithm is the basis and premise of FH. Rapid detection and accurate judgment of interference signal types can improve the efficiency of cognitive module. Time domain energy detection algorithm can quickly detect the

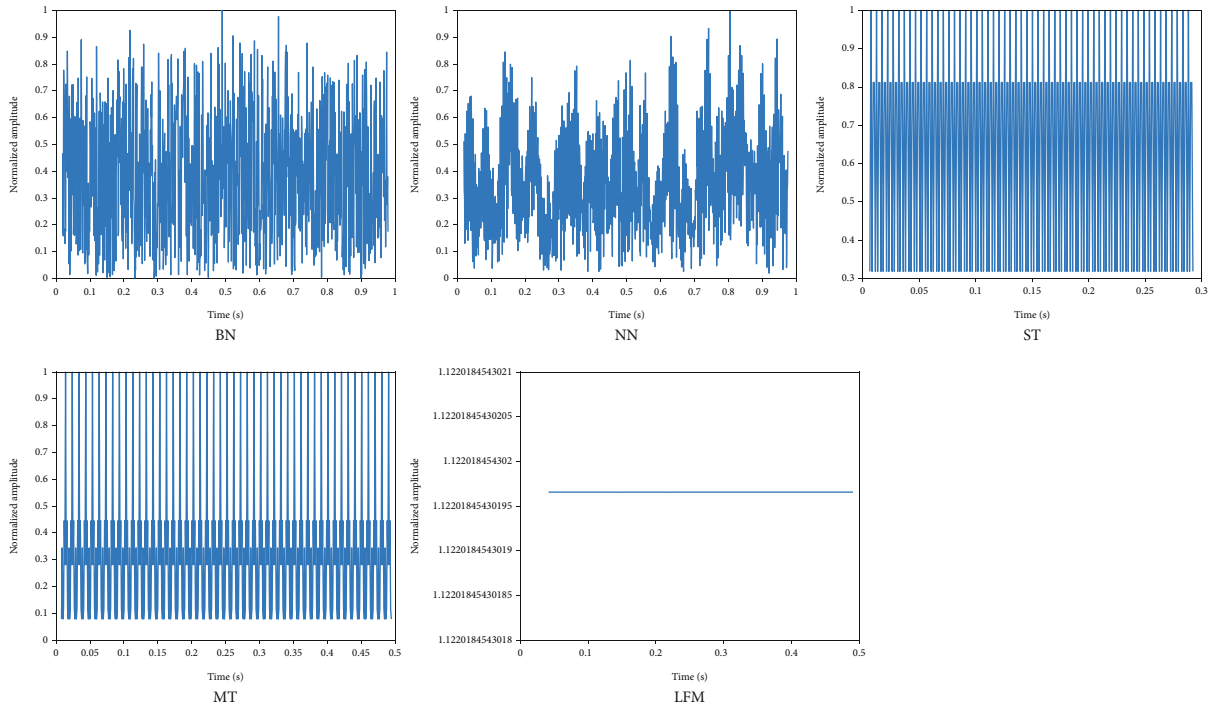

(a) Time domain diagrams

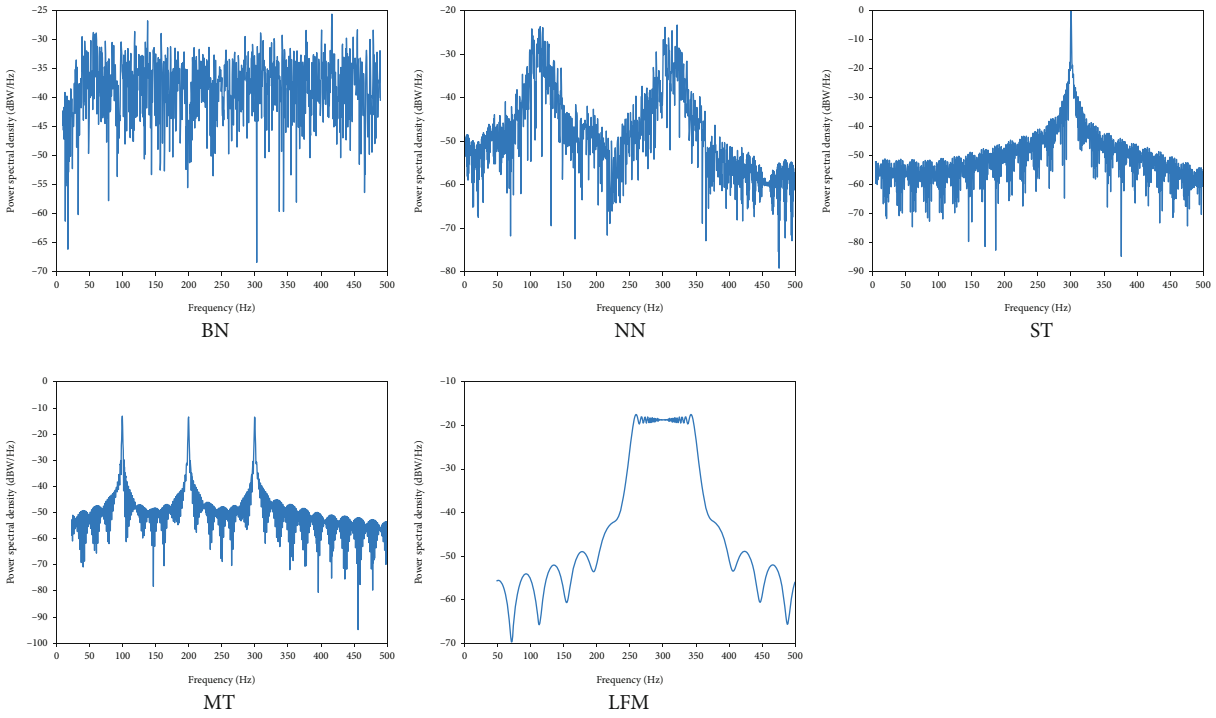

(b) Frequency domain diagrams

Figure 2: Time domain and frequency domain diagrams of typical interference.

presence of interference without the requirement of any prior information, which is easy to implement and widely applied. However, in addition to detecting the existence of interference, no more information can be obtained for time domain energy detection algorithm. Therefore, we adopt frequency domain detection algorithm to detect interference in this paper, which can locate interference frequency accurately.

The schematic diagram of frequency domain detection algorithm is shown in Figure 3. The signal was processed by A/D sampling and fast Fourier transform (FFT). Then, the sum square of the amplitude modulus of the frequency point is calculated and compared with the judgment threshold, in which way the position of interference frequency can be obtained. The judgment threshold is obtained by

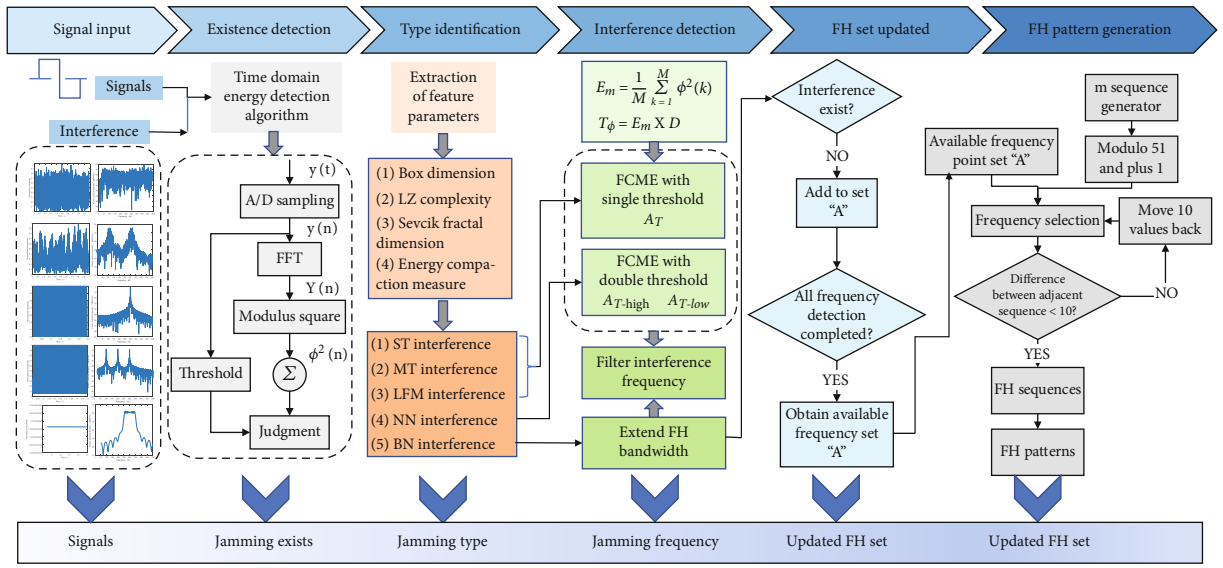

Figure 3: Data processing flow chart of cognitive FH system.

multiplying the threshold factor by the mean value of the noise spectral amplitude. However, the mean value of noise amplitude contains interference signals, which leads to an excessive threshold because the noise mean contains the interference signal. FCME algorithm can eliminate interference frequency points and constantly update the threshold to obtain the final judgment threshold. FCME algorithm improves the disadvantage of excessive threshold of frequency domain energy detection algorithm. We illustrate the detection performance of FCME algorithm with single threshold and double thresholds, respectively.

When calculating the detection threshold for the first time, FCME algorithm only considers a small part of the frequency points with small amplitude as noninterference signals. In this way, noise estimation accuracy is improved, and the value of threshold is more accurate. A/D sampling is performed on the received signal $y(t)$ to obtain $y(n)$, and FFT is performed to obtain $Y(n)$. The square of amplitude modulus at each frequency point of received signal can be expressed as follows:

$$\phi^2(n) = R_e^2|Y(n)| + I_m^2|Y(n)|, n = 0, 1, \cdots, N-1, \quad (10)$$

where the minor M values of $\phi^2(n)$ are noise frequency points, and the mean value is as follows:

$$E_m = \frac{1}{M}\sum_{k=1}^{M}\phi^2(k). \quad (11)$$

The judgment threshold T_ϕ is obtained by multiplying E_m with the threshold factor D as follows

$$T_\phi = E_m \times D. \quad (12)$$

The square of amplitude modulus $\phi^2(n)$ of remaining frequency points are compared with T_ϕ, and the frequency points greater than T_ϕ are considered to be interference frequency points. After eliminating the interference frequency points, the residual noise frequency points form a new set of noise frequency points. Repeating the algorithm above can continuously update the judgment threshold until no new interference frequency is removed. Therefore, the value of final detection threshold A_T is obtained. When the value of $\phi^2(n)$ is greater than A_T, it is determined as interference points. However, when FCME algorithm with single threshold detects discontinuous signals, such as NN interference, false alarm probability will be high or misjudged due to inappropriate threshold factors. Therefore, FCME algorithm with double thresholds is applied to NN interference detections.

FCME algorithm with double thresholds adopts two different threshold factors. The minor threshold factor is employed to detect all frequency points so that possible interference frequency points can be screened out. The set of selected interference frequency points is defined as cluster, using the larger threshold factor to detect the possible interference frequency in the cluster and ultimately determine whether there is interference. Specifically, $Y(n)$ is obtained by FFT of $y(t)$. Square of amplitude modulus $\phi^2(n)$ at each frequency point of received signal are expressed as follows:

$$\phi^2(n) = R_e^2|Y(n)| + I_m^2|Y(n)|, n = 0, 1, \cdots, N-1. \quad (13)$$

The minor M points are considered as frequency points which contain only noise and the average E_{m1} as follows:

$$E_{m1} = \frac{1}{M}\sum_{k=1}^{M}\phi^2(k). \quad (14)$$

The minor judgment threshold $T_{\phi 1}$ is obtained by multiplying the threshold factor D_1 with the mean value E_{m1} as follows:

$$T_{\phi 1} = E_{m1} \times D_1. \quad (15)$$

As mentioned above, the judgment threshold is continuously updated until no new interference frequency points are eliminated. The final judgment threshold is obtained as $A_{T-\text{low}}$. The higher threshold $A_{T-\text{high}}$ is obtained by multiplying the larger threshold D_2 with the mean square of the final amplitude modulus. Comparing the maximum value of each cluster with $A_{T-\text{high}}$, if it is greater than A, it is considered that this cluster is an interference frequency band.

3. Cognitive FH Strategy for UAV Swarms

As demonstrated above, frequency points which are interference can be screened out by FCME algorithms. Based on interference detection technology, we apply cognitive FH technology to the data link of UAV swarm. For UAV swarms, different communication channels for each UAV result in different and irregular interference frequency points. Conventional FH technology is difficult to meet the anti-interference requirements of each UAV. Cognitive FH technology can avoid interference frequency actively and possess excellent anti-interference effect. For cognitive FH strategy of UAV swarms, the system model and functional module will be introduced, respectively, in this section. The data processing flow chart of cognitive FH system is shown in Figure 3, including interference existence detection, interference type detection, interference frequency detection, FH set update, and FH pattern generation. In recent years, signal recognition based on deep learning has become a research hotspot [28, 29]. In addition, the complexity of signal recognition can be reduced by feature extraction [30]. Recognition algorithm based on Sevcik fractal dimension and energy aggregation degree obtains obvious advantages at low values of JNR, such as the fast recognition speed and high recognition rate [12]. The selection of FCME algorithm with single/double thresholds requires accurate interference identification results. Therefore, we adopt and we select two-dimensional feature interference recognition algorithm based on Sevcik fractal dimension and energy aggregation degree for the identification of signal type.

3.1. System Model. Cognitive FH strategy draws on the idea of cognitive radio and adds cognitive units to the conventional FH system. The data link employed for UAV swarms in this paper refers to link16 data link, and the system model for data link of UAV swarm based on cognitive FH is shown in Figure 3. Information from the transmitter is processed by Reed Solomon (RS) encoding, interleaving, cyclic code shift keying (CCSK) spread spectrum, and minimum shift keying (MSK) modulation. FH modulation is acquired by mixing frequency with frequency synthesizer output controlled by pseudorandom sequence. At the receiving terminal, compared with conventional FH technology, cognitive FH technology adds cognitive units for anti-interference. Therefore, the receiver can filter out the interference frequency by cognitive unit and update FH set. In addition, the receiver will decode, demodulate, despread, and deinterleave the received signal to get the original information.

As shown in Figure 3, the cognitive unit consists of interference cognitive module, cognitive decision module, and spectrum dynamic allocation module. Interference cognition module consists of interference detection and interference type recognition, which requires rapid and effective detection of interference signals from complex electromagnetic environment. Then, the interference type is determined and submitted to the cognitive decision module. Cognitive decision module makes corresponding anti-interference strategy based on interference information and filter interference frequency points. After obtaining the available FH points, they are transmitted to the dynamic spectrum allocation module to generate the available frequency hopping set. Finally, the updated FH frequency set is transmitted to the transmitter and receiver to optimize the FH system.

For the cognitive unit, the flow chart of signal processing is shown in Figure 4. First of all, energy detection algorithm is adopted to detect the presence of interference. Energy detection algorithm possesses high detection efficiency for preliminary screening of interference signals. Two characteristic parameters are extracted to form two-dimensional feature vector $\mathbf{T}$ when interference exists. $\mathbf{T}$ consists of frequency domain Sevcik fractal dimension and fractional Fourier domain energy aggregation degree, which is considered as the basis for interference identification. Then, recognition results are passed to the cognitive decision module. Cognitive decision module selects corresponding transmission strategy by interference type. When ST, MT, and LFM interference are identified, FCME with double thresholds obtains no obvious improvement compared to FCME with single threshold. Therefore, to reduce the detection delay and improve the real-time performance of the detection algorithm, FCME, the single threshold algorithm is selected to filter interference frequency. Similarly, when NN interference and BN interference are identified, FCME algorithm with double thresholds and FH bandwidth extension are adopted, respectively.

3.2. Functional Module. In this paper, 51 frequency points are selected and numbered as $1, 2, L \cdots, 51$ to constitute the initial frequency set. In addition, FH frequency range is set as 969~1008 MHz, 1053~1065 MHz, and 1113~1206 MHz, and frequency interval is set as 3 MHz.

When interference is detected, including ST, MT, LFM, NN, and BN interference, the system selects available frequency points from all frequency points for FH and updates the hopping frequency set. The flow chart of adaptive update for cognitive FH strategy can be seen in Figure 3. According to the results of interference identification, FCME algorithm with single or double thresholds is adopted to detect whether there is interference at each frequency point. If no interference exists, the frequency point number is added to set A. After all subband detection is completed, the FH frequency set is updated adequately.

The flow chart of FH pattern generation is demonstrated in Figure 5. Signals sent at the transmitter $s(t)$ can be expressed as follows:

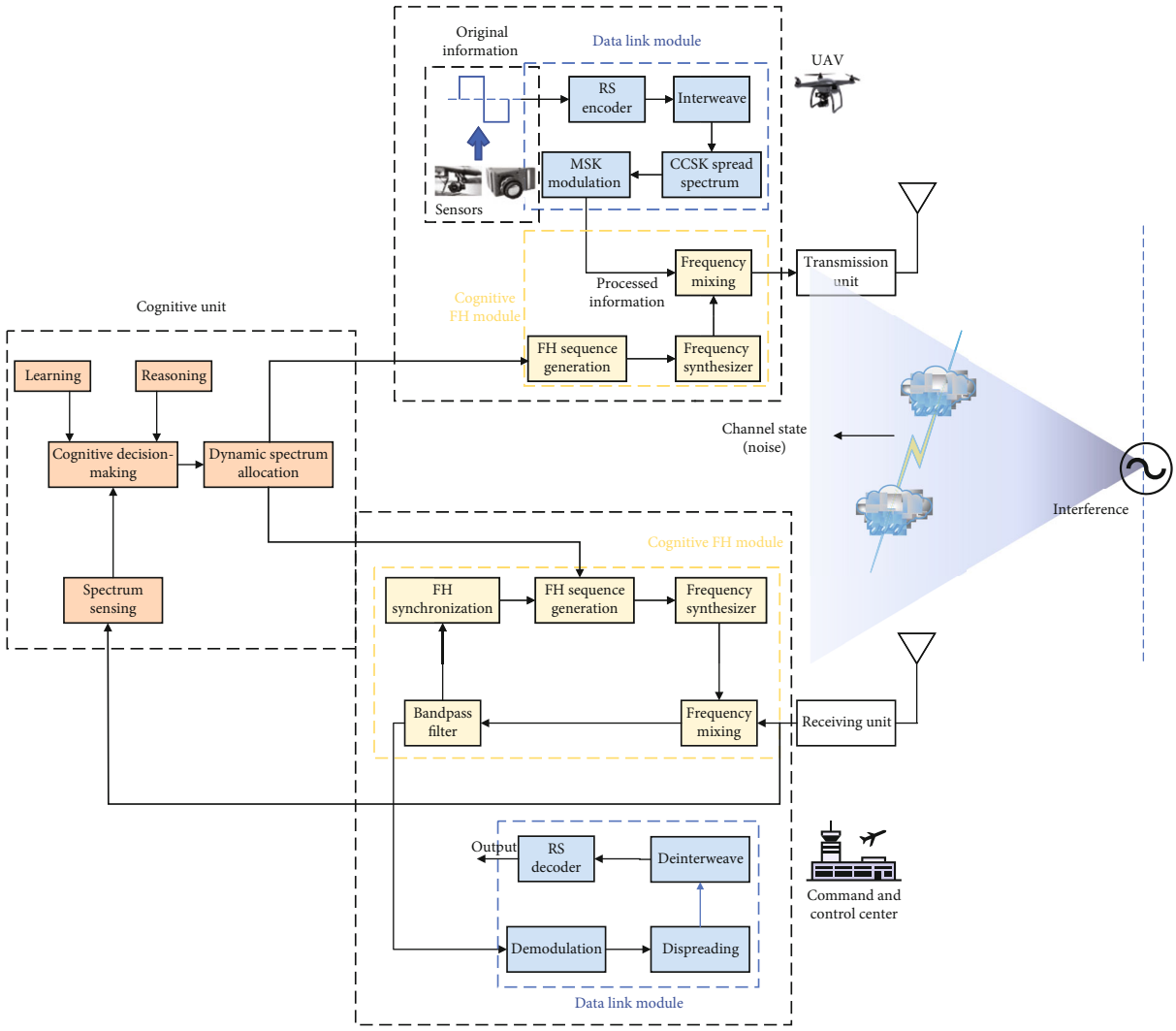

Figure 4: System model for data link of UAV swarm based on cognitive FH.

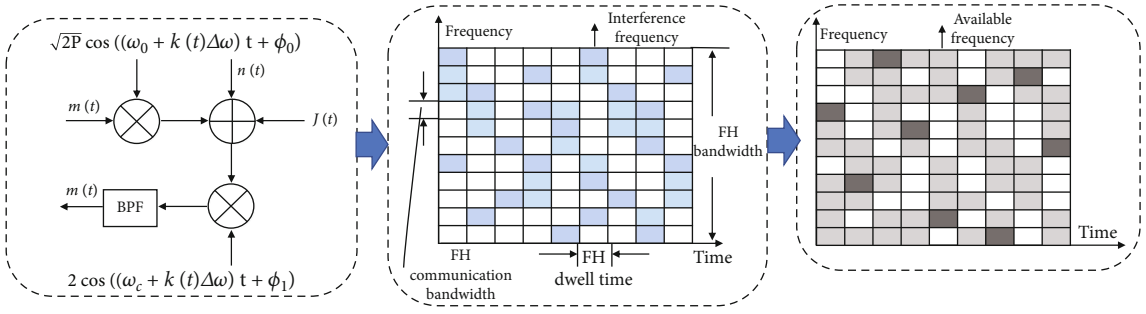

Figure 5: Flow chart of FH pattern generation.

$$s(t) = \sqrt{2P}m(t)\cos\left[(\omega_0 + k(t)\Delta\omega)t + \varphi_0\right], \quad (16)$$

$$r(t) = \sqrt{2P_i}m(t)\cos\left[(\omega_0 + k(t)\Delta\omega)t + \varphi(t)\right] + J(t) + n(t), \quad (17)$$

where $s(t)$ is modulated signals, ω_0 is minimum angular frequency, $\Delta\omega$ is the minimum interval of angular frequency, φ_0 is the initial phase, and $k(t)$ varies with pseudorandom sequence. In addition, signals received at the receiving terminal $r(t)$ can be expressed as follows:

where $J(t)$ and $n(t)$ represent interference signals and noise signals in channels, respectively. P_i is the power of the receiving signal, and $\varphi(t)$ represents the phase of the receiving signals.

When the FH synchronization is completed, the output of the mixer unit $r'(t)$ can be expressed as follows:

$$\begin{aligned} r'(t) &= r(t) \times 2\cos\{[(\omega_c + k(t)\Delta\omega)t + \varphi_1]\} \\ &= 2\sqrt{2P_i}m(t)\cos[(\omega_0 + k(t)\Delta\omega)t + \varphi(t)]\cos \\ &\quad \cdot [(\omega_c + k(t)\Delta\omega)t + \varphi_1] + 2[J(t) + n(t)]\cos \\ &\quad \cdot [(\omega_c + k(t)\Delta\omega)t + \varphi_1] \\ &= \sqrt{2P_i}m(t)\cos[\omega_I t + \varphi(t) - \varphi_1] \\ &\quad + \sqrt{2P_i}m(t)\cos\{[\omega_0 + \omega_c + 2k(t)\Delta\omega]t + \varphi(t) + \varphi_1\} \\ &\quad + 2[J(t) + n(t)]\cos[(\omega_c + k(t)\Delta\omega)t + \varphi_1], \end{aligned} \tag{18}$$

where $2\cos\{[(\omega_c + k(t)\Delta\omega)t + \varphi_1]\}$ is output of the frequency synthesizer, ω_c is the central angular frequency, φ_1 is phase deviation, ω_I is intermediate frequency angular frequency, and $\omega_I = \omega_c - \omega_0$. The output signal of band-pass filter (BPF) $m'(t)$ can be expressed as follows:

$$m'(t) = \sqrt{2P_i}s(t)\cos[\omega_I t + \varphi(t) - \varphi_1] + J'(t) + n'(t), \tag{19}$$

where $J'(t)$ and $n'(t)$ represent interference and noise at the output end.

Different from the conventional FH technology which selects the FH carrier frequency from all frequency points, cognitive FH adopts frequency points from the updated available hopping frequency set according to the results of interference frequency selections. In addition, the interval between adjacent frequency points is more than 30 MHz. As depicted in Figure 5, the blue part, grey part, and black part represent interference frequency, available frequency, and the selected frequency. The available frequency set A can be expressed as follows:

$$A = A_E - A_I = \{f_i | f_i \in A_E, f \notin A_I\}, \tag{20}$$

where A, A_E, and A_I express the available frequency set, the entire frequency set, and the removed frequency set. After completing the adaptive update of the FH set, a set of available frequency hopping points A is obtained. Then, the FH sequence is generated by employing m sequence with length of 63. The obtained FH sequence is taken as modulus 51 and add 1, in which way the FH sequence between 1 and 51 can be acquired. In order to make the interval between adjacent FH points not less than 30 MHz, the difference between adjacent FH sequences should be guaranteed more than 10.

At the receiving terminal, cognitive unit of cognitive FH strategy obtains the available FH set through perception, analysis, and decision-making. Then, cognitive FH transmits relevant information to both transmitter and receiver through a reliable public communication channel. Therefore, the transmitter and the receiver obtain the same spectrum information and realize FH synchronization and communication parameters adjustment.

4. Numerical Results and Analysis

In the cognitive FH strategy data link of this paper, transmission slots of the system are divided into data transmission slot and interference cognitive time slots, which are carried out alternately. The interference cognition takes up one FH time slot, and the data transmission occupies 93 FH time slots. We assume that the cognitive FH strategy of UAV swarm is applied in open plains with less obstacles, such as mountains and buildings. Therefore, the Nakagami-m channel fading model is selected for simulations, where the value of parameter m represents the severity of fading. Specifically, it can be considered as Rayleigh fading channel when $m = 1$, Rice channel when $m > 1$, and AWGN channel when $m \longrightarrow \infty$. Considering that the scenario for UAV data link in this paper is a broad plain environment, the value of m is set to 2. Other simulation parameters refer to link 16 in this paper, and specific parameter settings are shown in Table 1.

We have simulated BER performance of five typical types of interference of different values of JNR, including BN interference, NN interference, ST interference, MT interference, and LFM interference. We adopt JNR = 12dB , JNR = 8dB, JNR = 4dB, and JNR = 0dB for simulations. BER performance of different values of JNR for BN interference is shown in Figure 6. BN interference is realized by applying interference to the whole bandwidth of FH communications. It can be seen that at the same value of SNR, larger value of JNR leads to worse BER performance. Larger values of JNR lead to greater interference power and the interference power allocated to each frequency point is greater, which generate greater damage to the communication system. Therefore, countering BN interference can be achieved by extending hopping bandwidth because wider bandwidth increases the difficulty of interference. In addition, BER performance of cognitive FH strategy is superior to conventional FH system. For example, when BER = 10^{-3} and JNR = 8dB, cognitive FH strategy obtains 1 dB gains compared to conventional FH system. Hence, cognitive FH system improves the ability of UAV data link against BN interference.

As mentioned above, FCME with double thresholds obtains better detection performance for NN interference. Therefore, FCME with double thresholds is selected to remove the frequency points with interference and update FH set for NN interference system. The BER performance of different JNR for NN interference system is shown in Figure 7. NN interference in simulations contains two interference bands. It can be seen that cognitive FH attains better BER performance compared to conventional FH systems when the value of JNR is fixed. Specifically, when the values of BER and JNR are 10^{-4} and 4 dB, cognitive FH strategy obtains approximately 0.2 dB gains compared to conventional FH system.

Tone interference includes ST interference and MT interference. FCME with single threshold achieves satisfactory detection results and filter out interference. Since FCME with double thresholds does not obviously improve detection performance compared to FCME with single threshold,

Table 1: Parameters for simulations.

Frequency range	969~1008 MHz, 1053~1065 MHz, 1113~1206 MHz
Coding mode	RS (31, 15)
Modulation mode	MSK
Spread Spectrum mode	CCSK (32, 5)
Frequency interval	3 MHz
FH interval	30 MHz
FH points	51

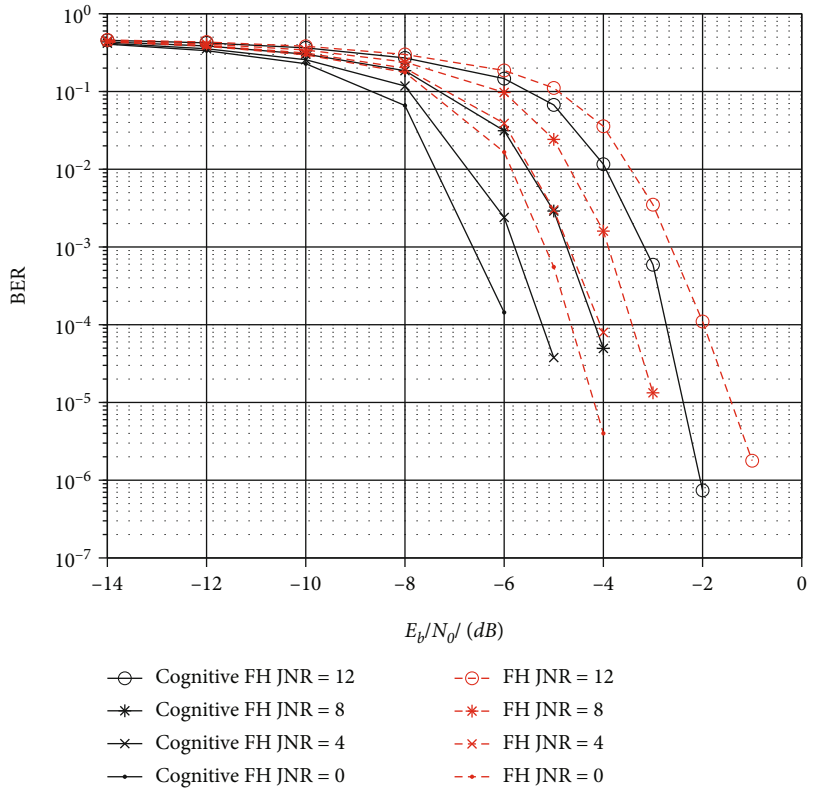

Figure 6: BER performance of different JNR for BN interference.

to reduce the detection delay and enhance the real-time performance of the detection algorithm, FCME with single threshold is adopted. BER performance of different JNR for ST interference is depicted in Figure 8. For conventional FH system, BER performance reduces as the value of JNR decreases because it cannot avoid interference points. However, BER performance of cognitive FH strategy has no obvious change with the different values of JNR. As a routine means of interference, tone interference can be detected by FCME algorithm, and interference can be filtered out easily. Therefore, cognitive FH strategy obtains better BER performance compared to conventional FH system for ST interference.

BER performance of different JNR for MT interference is depicted in Figure 9. Similar to ST interference, MT interference can also find interference frequency points accurately through FCME algorithm and eliminate interference frequency points. Simulation results indicate that cognitive FH strategy attains better BER performance than conventional FH system especially when the value of JNR is high. Therefore, cognitive FH can obviously improve BER performance for MT interference.

LFM interference is to scan the entire communication frequency band with a signal with relatively narrow bandwidth within a certain time. The instantaneous state of LFM can be regarded as NN interference. Therefore, we adopt FCME algorithm to detect and update FH set. BER performance of different JNR for LFM interference is shown in Figure 10, and the interference bandwidth is set to 30 MHz. BER performance of different JNR values is obviously different for cognitive FH strategy because FCME algorithm cannot detect all interference frequency points. Cognitive FH obtains better performance compared to conventional FH, but cognitive FH strategy cannot remove all interference frequency since LFM is a sweep interference.

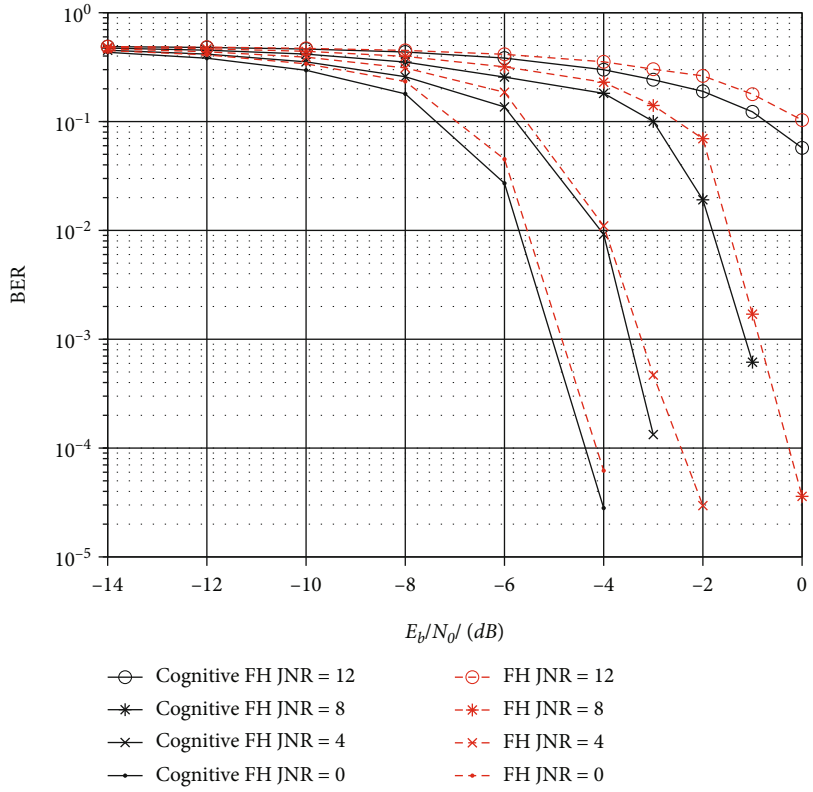

Figure 7: BER performance of different JNR for NN interference.

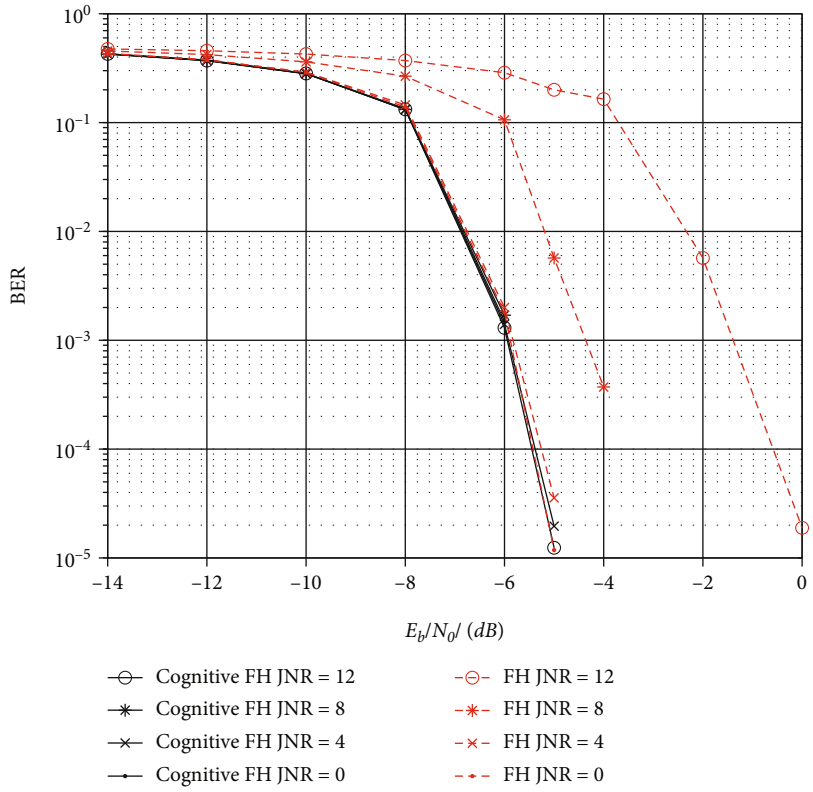

Figure 8: BER performance of different JNR for ST interference.

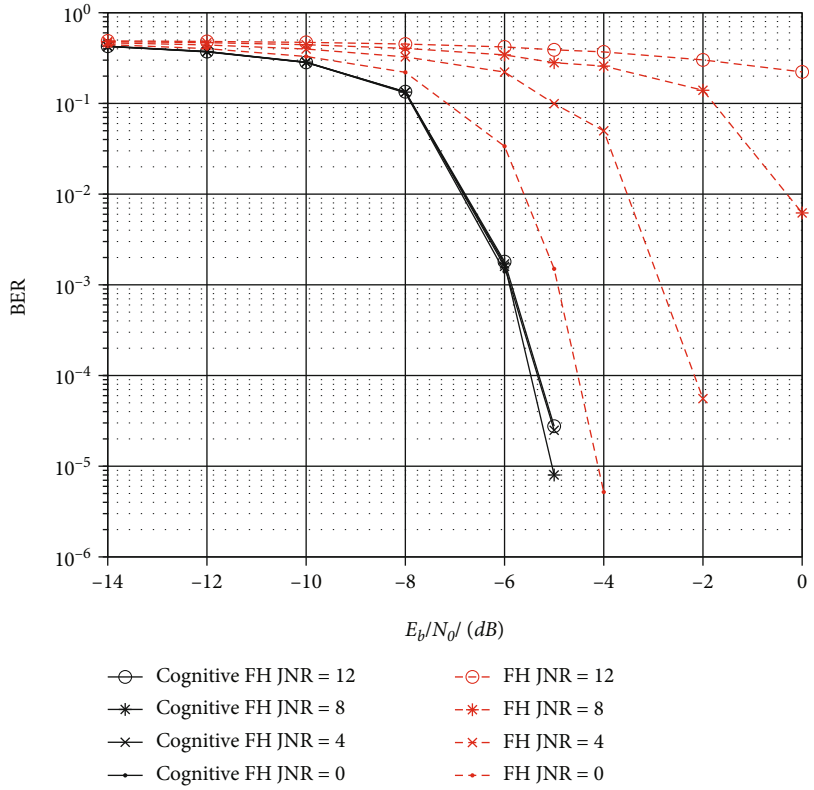

Figure 9: BER performance of different JNR for MT interference.

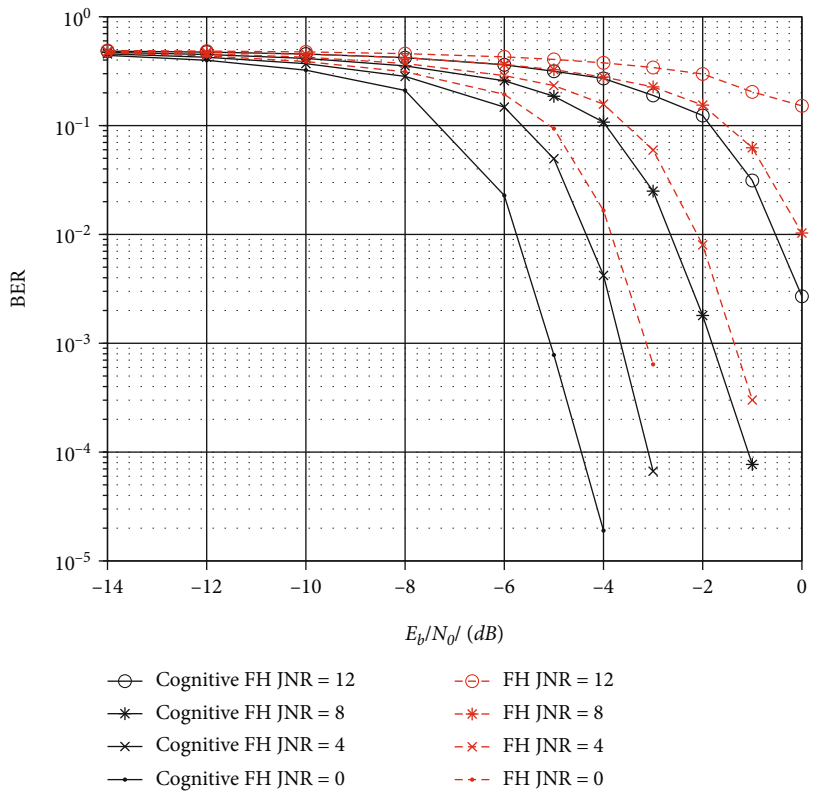

Figure 10: BER performance of different JNR for LFM interference.

5. Conclusions

To improve the robustness for data link of UAV swarm, this paper proposed cognitive-based high robustness frequency hopping strategy in complex electromagnetic environment. Through detecting and identifying the interference, the proposed cognitive FH strategy can obtain the type of interference and interference frequency points. Afterwards, the cognitive FH strategy can actively avoid the interference frequency points by updating the FH frequency set. Simulation results show that BER performance of cognitive FH strategy is improved compared to conventional FH system for five different types of interference, including BN interference, NN interference, ST interference, MT interference, and LFM interference. For example, when the value of target BER is 10^{-3}, cognitive FH strategy obtains approximately 0.5 dB gains of NN interference for different JNR values compared to conventional FH system. Cognitive FH strategy can adaptively select anti-interference strategy according to actual conditions, which enhances robustness for UAV swarms. In the future, electromagnetic environment faced by UAV swarms will be more complicated, which leads to an increasing requirement for anti-interference ability of the system. Therefore, cognitive FH strategy will become an important component for the data link of UAV swarms.

Data Availability

No data were used to support this study.

Conflicts of Interest

The authors declare that there are no conflicts of interest regarding the publication of this paper.

Acknowledgments

This paper was supported in part by the National Natural Science Foundation of China (No. 61873070), the Heilongjiang Provincial Natural Science Foundation of China (No. LH2020F018), and the Fundamental Research Funds for the Central Universities (No. 3072022QBZ0803).

References

[1] J. Liu, N. Sha, W. Yang, J. Tu, and L. Yang, "Hierarchical q-learning based uav secure communication against multiple UAV adaptive eavesdroppers," *Wireless Communications and Mobile Computing*, vol. 2020, Article ID 8825120, 15 pages, 2020.

[2] H. Niu, X. Zhao, L. Hou, and D. Ma, "Energy efficiency maximization for UAV-assisted emergency communication networks," *Wireless Communications and Mobile Computing*, vol. 2021, Article ID 7595347, 15 pages, 2021.

[3] R. Xue, M. Zhao, and H. Tang, "Information transmission schemes based on adaptive coded modulation for UAV surveillance systems with satellite relays," *IEEE Access*, vol. 8, no. 8, pp. 191355–191364, 2020.

[4] B. Li, Z. Fei, and Y. Zhang, "UAV communications for 5G and beyond: recent advances and future trends," *IEEE Internet of Things Journal*, vol. 6, no. 2, pp. 2241–2263, 2018.

[5] M. M. Azari, G. Geraci, A. Garcia-Rodriguez, and S. Pollin, "UAV-to-UAV communications in cellular networks," *IEEE Transactions on Wireless Communications*, vol. 19, no. 9, pp. 6130–6144, 2020.

[6] A. Mukherjee, S. Misra, A. Sukrutha, and N. S. Raghuwanshi, "Distributed aerial processing for IoT-based edge UAV swarms in smart farming," *Computer Networks*, vol. 167, article 107038, 2020.

[7] X. Chen, J. Tang, and S. Lao, "Review of unmanned aerial vehicle swarm communication architectures and routing protocols," *Applied Sciences*, vol. 10, no. 10, article 3661, 2020.

[8] J. Wang, Y. Liu, S. Niu, and H. Song, "Extensive throughput enhancement for 5G-enabled UAV swarm networking," *IEEE Journal on Miniaturization for Air and Space Systems*, vol. 2, no. 4, pp. 199–208, 2021.

[9] M. Liu, Z. Liu, W. Lu, Y. Chen, X. Gao, and N. Zhao, "Distributed few-shot learning for intelligent recognition of communication jamming," *IEEE Journal of Selected Topics in Signal Processing*, vol. 16, no. 3, pp. 395–405, 2022.

[10] Z. Bao, Y. Lin, S. Zhang, Z. Li, and S. Mao, "Threat of adversarial attacks on DL-based IoT device identification," *IEEE Internet of Things Journal*, vol. 9, no. 11, pp. 9012–9024, 2022.

[11] L. Lin, C. Chen, K. Su, B. Chen, and H. Li, "Design of anti-interference system for fully autonomous UAV based on ADRC-EKF algorithm," in *2019 IEEE 2nd International Conference on Electronics and Communication Engineering (ICECE)*, pp. 428–433, Harbin, China, 2019.

[12] R. Xue, J. Liu, and H. Tang, "Two-dimensional jamming recognition algorithm based on the Sevcik fractal dimension and energy concentration property for UAV frequency hopping systems," *Information*, vol. 11, no. 11, p. 520, 2020.

[13] W. Wang, B. Jiang, X. Tan, and C. Li, "UAV communication interference analysis and anti-interference methods," in *Proceedings of the 2020 International Conference on Cyberspace Innovation of Advanced Technologies*, pp. 197–201, Guangzhou, China, 2020.

[14] H. Baek and J. Lim, "Design of future UAV-relay tactical data link for reliable UAV control and situational awareness," *IEEE Communications Magazine*, vol. 56, no. 10, pp. 144–150, 2018.

[15] Y. Zheng, S. Li, K. Xing, and X. Zhang, "Unmanned aerial vehicles for magnetic surveys: a review on platform selection and interference suppression," *Drones*, vol. 5, no. 3, p. 93, 2021.

[16] S. Yan, M. Peng, and X. Cao, "A game theory approach for joint access selection and resource allocation in UAV assisted IoT communication networks," *IEEE Internet of Things Journal*, vol. 6, no. 2, pp. 1663–1674, 2018.

[17] S. Popli, R. K. Jha, and S. Jain, "Green NOMA assisted NB-IoT based urban farming in multistory buildings," *Computer Networks*, vol. 199, article 108410, 2021.

[18] M. Shalaby, M. Shokair, and N. W. Messiha, "Modelling and simulation of narrow band electromagnetic interference in millimeter wave massive MIMO systems," in *2018 35th National Radio Science Conference (NRSC)*, pp. 149–156, Cairo, Egypt, 2018.

[19] Y. He, D. Zhai, R. Zhang, X. du, and M. Guizani, "An anti-interference scheme for UAV data links in air–ground integrated vehicular networks," *Sensors*, vol. 19, no. 21, p. 4742, 2019.

[20] Z. Wang, R. Liu, Q. Liu, L. Han, and J. S. Thompson, "Feasibility study of UAV-assisted anti-jamming positioning," *IEEE Transactions on Vehicular Technology*, vol. 70, no. 8, pp. 7718–7733, 2021.

[21] G. Shichao, G. Dandan, Z. Qiongyu, W. Nankai, and D. Jiaxin, "Research progress of anti-jamming technology of unmanned aerial vehicle (UAV) data link," *IOP Conference Series: Materials Science and Engineering*, vol. 816, article 012011, 2020.

[22] B. M. Todorovic and V. D. Orlic, "Direct sequence spread spectrum scheme for an unmanned aerial vehicle PPM control signal protection," *IEEE Communications Letters*, vol. 13, no. 10, pp. 727–729, 2009.

[23] Y. Tu, Y. Lin, H. Zha et al., "Large-scale real-world radio signal recognition with deep learning," *Chinese Journal of Aeronautics*, 2021.

[24] M. Liu, C. Liu, M. Li, Y. Chen, S. Zheng, and N. Zhao, "Intelligent passive detection of aerial target in space-air-ground integrated networks," *China Communications*, vol. 19, no. 1, pp. 52–63, 2022.

[25] S. Xie and B. Qian, "Performance analysis of differential frequency hopping communication system over Rician channel," in *2018 IEEE 4th Information Technology and Mechatronics Engineering Conference (ITOEC)*, pp. 1015–1019, Chongqing, China, 2018.

[26] J. Peng, Z. Zhang, Q. Wu, and B. Zhang, "Anti-jamming communications in UAV swarms: a reinforcement learning approach," *IEEE Access*, vol. 7, pp. 180532–180543, 2019.

[27] K. Li, C. Wang, M. Lei, M.-M. Zhao, and M.-J. Zhao, "A local reaction anti-jamming scheme for UAV swarms," in *2020 IEEE 92nd Vehicular Technology Conference (VTC2020-Fall)*, pp. 1–6, Victoria, BC, Canada, 2021.

[28] Y. Lin, H. Zhao, X. Ma, Y. Tu, and M. Wang, "Adversarial attacks in modulation recognition with convolutional neural networks," *IEEE Transactions on Reliability*, vol. 70, no. 1, pp. 389–401, 2021.

[29] Y. Lin, Y. Tu, and Z. Dou, "An improved neural network pruning technology for automatic modulation classification in edge devices," *IEEE Transactions on Vehicular Technology*, vol. 69, no. 5, pp. 5703–5706, 2020.

[30] M. Liu, J. Wang, N. Zhao, Y. Chen, H. Song, and R. Yu, "Radio frequency fingerprint collaborative intelligent identification using incremental learning," *IEEE Transactions on Network Science and Engineering*, 2021.